Solid Freeform Fabrication 2017: Proceedings of the 28th Annual International Solid Freeform Fabrication Symposium – An Additive Manufacturing Conference
Reviewed Paper

CONTROLLING THERMAL EXPANSION WITH LATTICE STRUCTURES USING LASER POWDER BED FUSION

S.S. Milward[1], H. Swygart[2], L. Eccles[2], S.G.R. Brown[1], N. P. Lavery[1]

[1]College of Engineering, Swansea University Bay Campus, Wales, SA20AB
[2]Qioptiq, Glascoed Road, Saint Asaph, LL17 0LL

Abstract

Tuning the Co-efficient of Thermal Expansion (CTE) of a component is traditionally limited by material choice. Laser Powder Bed Fusion (LPBF) enables the designer to create complex geometries including lattice structures. When combined with a secondary material, these metallic lattice structures can be designed to exhibit different CTE's whilst retaining stiffness. This allows the designer the freedom to adjust the CTE by changing CAD variables such as lattice angle, and member thicknesses.
This paper aims to develop an arrangement for CTE matched components for high precision optical systems. Development pursued using a Static Thermo-Structural Finite Element Analysis model to determine the best arrangements for the required CTE change.
The results are incorporated into a new design prototype of a full cylindrical lens system in metal on a Laser Powder Bed Fusion machine.

Introduction

Additive Layer Manufacturing (ALM) has provided companies with an ability to quickly create functional parts with a range of materials from metals to plastics. Companies are increasingly looking into new ways to save money on tool up costs for low volume components. This makes ALM a very attractive proposition for the industry. Alongside the obvious benefits of ALM, comes its ability to create lattice structures. Typical lattice structures used in the industry today consist of standardised arrangements of struts which are mostly used to fill in voids or in place of solid material. This helps save on weight and material costs, and can be generated by most software in the commercial and industrial markets. They are beneficial for an industry which takes weight reduction seriously, such as the aerospace, defence, and automotive industry. In 2017 Thales Alenia used metal ALM to produce 79 metal parts for Tlkon 3S, SGDC, and KOREASAT-8. Many other companies have also created parts for satellites, aeroplanes and rockets [1]. In 2011 Astrium created titanium EBM parts for the Atlantic Bird 7 satellite which saved 30% mass compared to traditional manufacturing means. This was achieved using lattice infill structures and topology optimisation techniques that lend themselves to ALM [2]. Additional functions can be added to play an active role in improving the characteristics of the part. These can range from the obvious such as weight reduction already actively used, to the more novel uses such as; impact absorption, thermal insulation, heat dissipation, and thermal expansion control. These have all been proven possible with unique geometries, which could lend themselves to manufacture and incorporation into existing ALM components [3][4][5]. This paper will look at how parts can be designed to provide specifically thermal expansion control, by utilising different lattice designs and ALM techniques.

Thermal expansion of components in an assembly is a design problem that has to be considered by most engineering industries. Issues arise when components experience a range of temperatures causing expansion and contraction, affecting its operational behaviour. Particular care has to be given when assembling multiple material parts due to different CTE values. These can cause expansion gaps, contact stresses, cycling fatigue, and component misalignment. The sponsor company Qioptiq has initiated a research program with the aim of improving the optical stability of their current and future systems. Qioptiq's components must withstand changes in temperature from -50°C to +70°C, all whilst maintaining strength, alignment, and a lightweight design. Particular care has to be given to products which enter space. In this environment, rapid changes of temperature occur without the possibility of cooling by convection. This can lead to severe thermal gradients, stresses, and distortion. Problems can occur in satellites where optical systems

may be present which require dimensional stability, or antennas where a low CTE is required for a precisely tuned waveband. Space applications are a future application for Qioptiq if the concept is proven successful. LPBF has been tested with low expansion alloys such as INVAR which exhibit a CTE in the region of $1.44x10^{-6}$(1/K). Due to the materials high density, topology optimisation can be used to reduce its mass, increasing its viability over traditional methods.

There are several methods for controlling the CTE of a component. The more traditional methods involve material composition adjustments. This can be achieved in INVAR by varying the percentage of nickel from 36% to 56% to obtain the required CTE of between $1\text{-}11x10^{-6}$(1/K). Additional elements can also be added to INVAR to change its CTE. Some variations on INVAR include KOVAR, a FeNiCo alloy designed to exhibit similar CTE's to that of borosilicate glass, useful in optical systems for applications such as satellites [6][7]. Variations in nickel percentage can affect mechanical properties which may be undesirable [8].

A new method is proposed which utilises the unique advantages of ALM to control the thermal expansion of an annulus surrounding a glass or germanium lens. This will allow Qioptiq to control the CTE between the lens material and its metal casing. In order to achieve this goal a unique structure will be developed, comprising two materials each exhibiting different coefficients of thermal expansion. The unique concept will allow Qioptiq's engineers to change the CTE in the design phase in CAD, by adjusting key dimensions of a bi-material lattice structure. One material must exhibit a higher CTE than the other to achieve an overall change in CTE. Integration into Qioptiq's existing designs would be advantageous, however tailored new designs for unique purposes are also being considered.

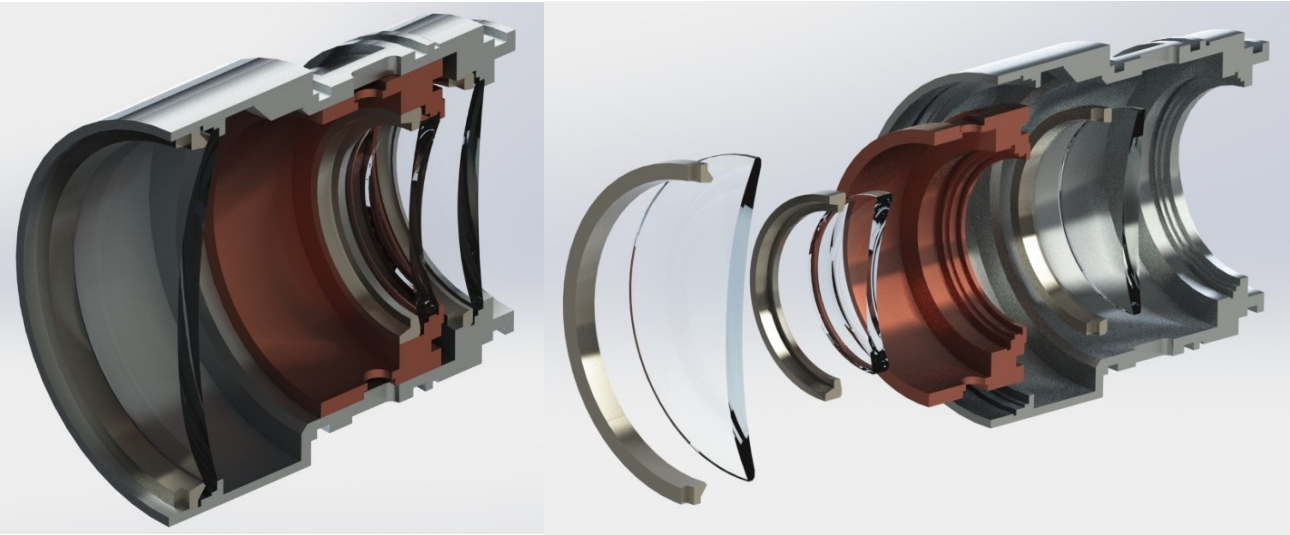

Figure 1) Image showing one example of an existing optical system supplied by Qioptiq.

LPBF solutions

When using LPBF only one material can be manufactured at a time, meaning two parts have to be assembled after manufacture. This design uses a single material lattice structure in combination with a secondary outer restraining ring from a lower CTE material such as INVAR. The inner lattice material will be shrink-cooled and inserted inside the INVAR ring. This solution is capable of creating a negative CTE when performing a Static Thermo-Structural FE Simulation with Titanium and INVAR over a temperature range of 100C.

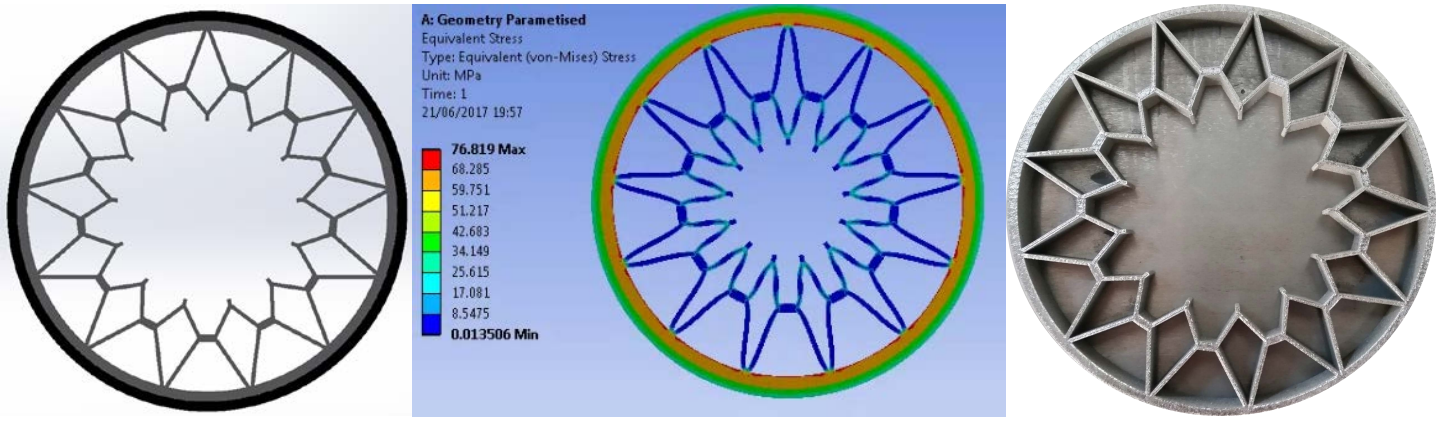

Figure 2- a) CAD Drawing showing a shrink-fitted outer low CTE ring with a higher CTE lattice structure. b) Von-Mises stress plot showing max stress distribution and a visual representation of deformation directions exaggerated by 300 times. C) Ti64Al manufactured with 45mm outer radius.

Single print solutions

Printing two materials together as one allows for the removal of the shrink fitting stage. It provides a greater level of design freedom where 3D structures can also be made, which opens up the possibility to control CTE in the third dimension.

A Direct Energy Deposition (DED) system such as a LENS® machine could be used to print the secondary lower CTE material in situ with the lattice structure. This system allows for the creation of bi-metallic structures using two blown powders simultaneously. This can allow for replication of 2D and 3D zero and negative CTE lattice structures such as those proposed by, Sigmund et al. 1996 [9], and Steeves et al 2007 [10] [11].

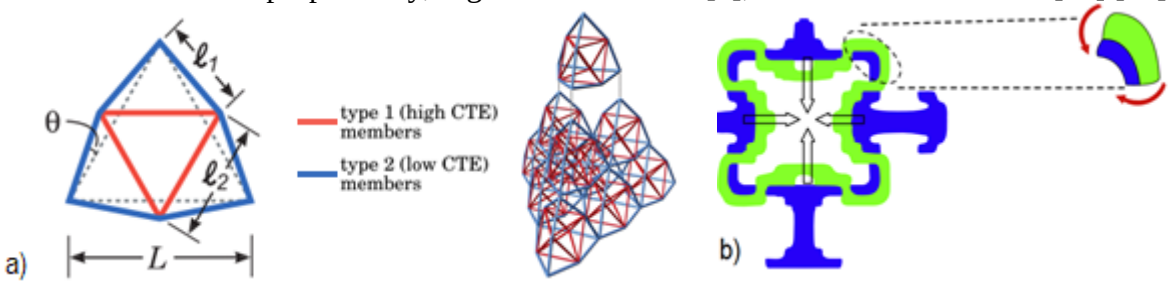

Figure 3a) Lattice structures proposed by Steeves showing high and low CTE constituents [10]. *b) Topologically optimised cell by Sigmund showing high CTE constituents in green and low CTE constituents in blue* [11].

The lattice structure used by Sigmund [11] was successfully printed using DED in nickel and chromium [5]. This can also be achieved with a polymer. Qang et. al. has made progress into 3D printing polyethylene glycol diacrylate (PEGDA) lattice structures with copper powder includes. The varying percentage of copper reinforcement up to 10% lowers the CTE from 1.56×10^{-1}(1/K) to 5.1×10^{-5}(1/K), a decrease of a third. This is enough to create a negative CTE over a 200K temperature range. The machine used is a customised form of Stereolithography [12]. DED using multiple materials is the next step to achieving a 3D structure with three-dimensional CTE control.

Development of FEA Models

An auxetic solution has been adapted for maximum thermal expansion change whilst maintaining stiffness. It can be seen that the expansion rate of the outer ring is limited; however the lattice structure is allowed to expand freely. This ensures that the adjoining material (labelled L2 in figure 5a) can expand freely and bend the two neighbouring members.
Both designs ensure that the angle on both lattices is equal to a tangential line, and thus maximum force is transmitted into the neighbouring structure. This is shown in figure 5a. During angle change, it is ensured that the radius of the inner annulus at Probe 1 is fixed, and the members change in length accordingly. Fixing this

radius is required for a specific lens diameter. When the angle θ changes, the diameter of the circle attached to the tangent line also increases. These probe locations are where the displacement will be measured from in the y-direction using a Static Thermo-Structural Finite Element Simulation in ANSYS. The displacement outputs can be used to calculate the CTE and stiffness using the equations below;

$$CTE = \frac{Displacement\ from\ probe\ 1}{(Radius\ at\ probe\ 1)\ X\ (Change\ in\ temperature)} \qquad Stiffness = \frac{Force\ applied\ in\ FEA}{Displacement\ from\ Probe\ 1}$$

Figure 6 provides a visual representation of the angle change from 50 to 75 degrees. This is the minimum and maximum angle that can be used, and its effect on the CTE will be analysed.
The materials used are INVAR with a CTE of $1x10^{-6}$(1/K), and Ti64Al with a CTE of $9.4x10^{-6}$(1/K).
In a separate simulation where the temperature is static, loads have also been placed normal to each structure around the annulus to determine its stiffness in the elastic region. The results have been plotted on a graph shown in figures 7 and 8.

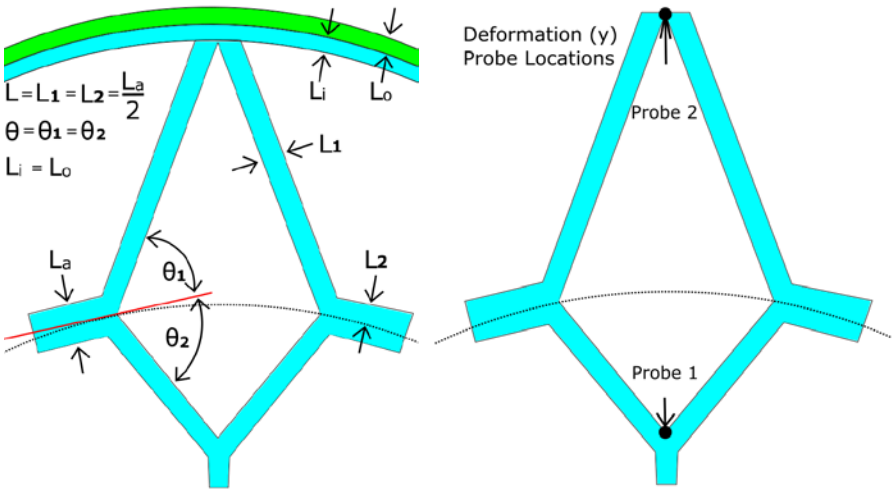

Figure 4a) Shows both equal angles theta on its most efficient tangential line. b) Figure showing ANSYS deformation probe locations used to take CTE and stiffness measurements.

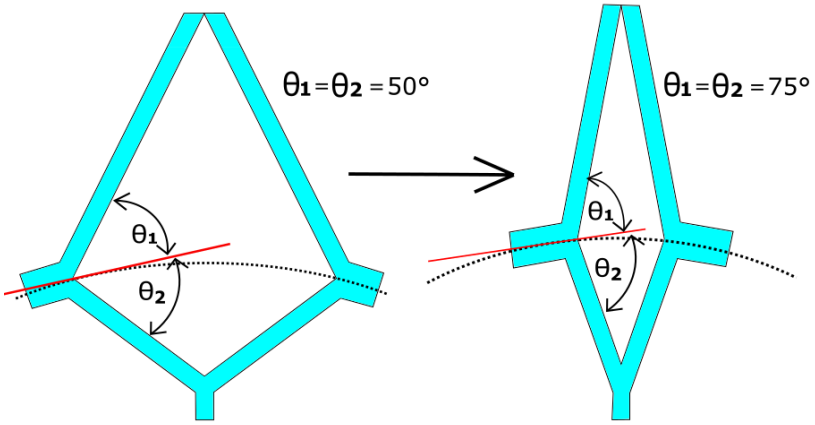

Figure 5) Shows the structure as it changes from the minimum to maximum angle.

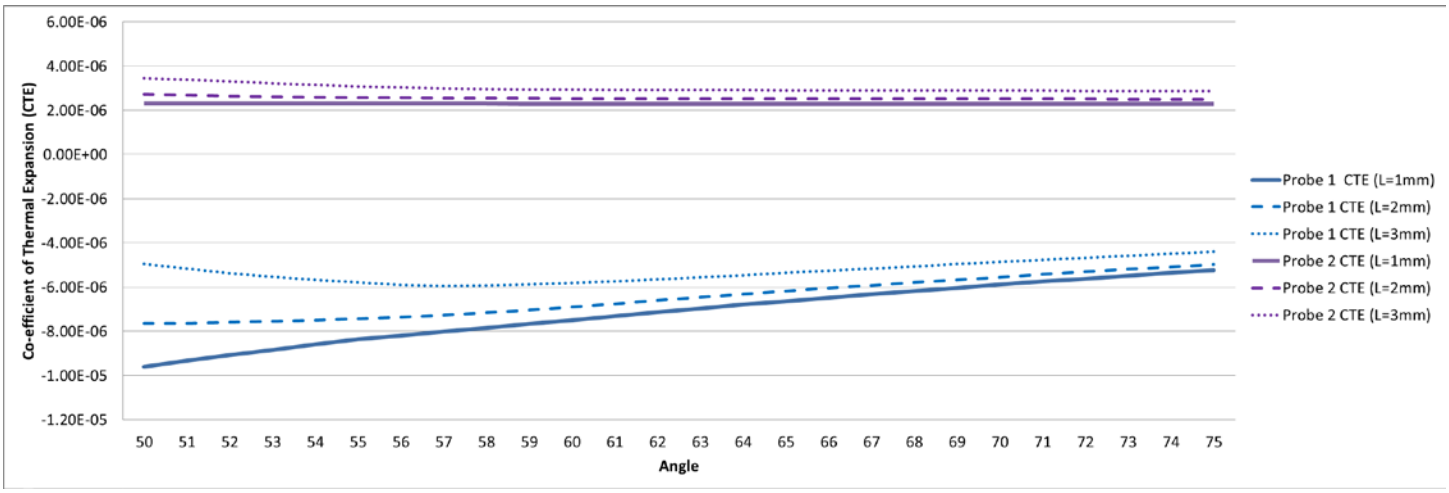

Figure 6) Graph showing simulation results of the CTE range as the angle (θ) of the lattice structure changes. Plots made for each member thicknesses (L, La).

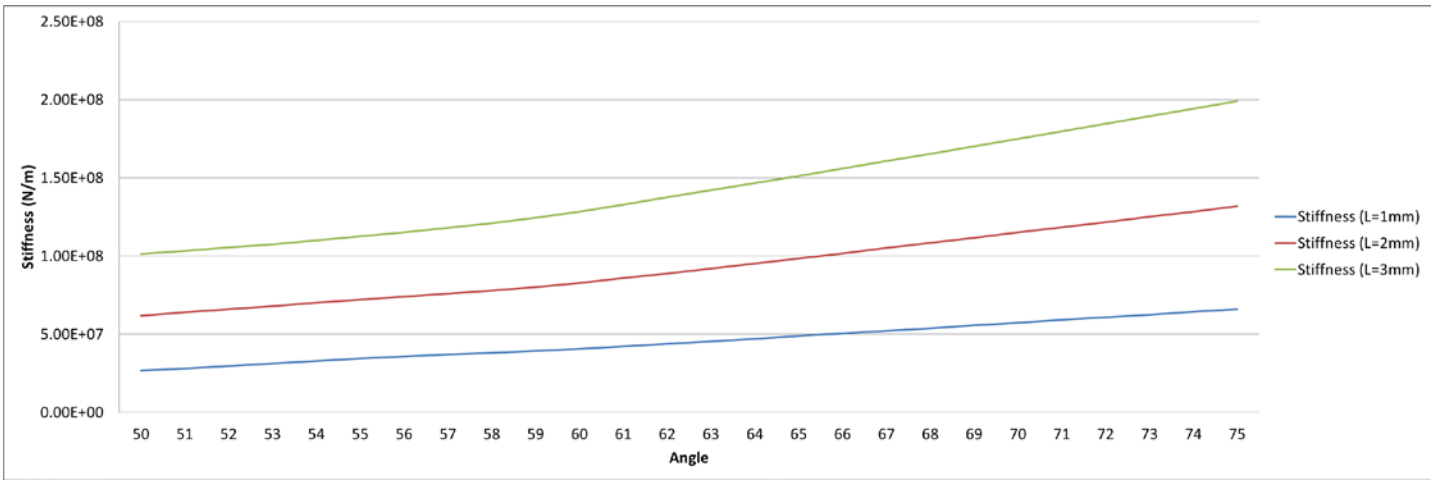

Figure 7) Graph showing simulation results of the stiffness in N/m as the lattice angle (θ) changes for each member thickness (L).

By analysing the simulation data it can be seen a negative CTE can be obtained using the lattice structure. In all member thicknesses, the CTE of the bi-metallic ring at probe 2 can be seen as relatively constant. The displacement at probe 2 is steady despite the angle change since the ring cannot move; only the lattice can move inwards due to its geometry. This can be seen in figure 2b). The difference between probe 1 and 2 denotes the effectiveness of the lattice structure. It can be seen that the increase in member thickness has not seen a dramatic change in CTE, but exhibits a far higher stiffness. This is a unique feature of the structure, since the adjoining material (La) is twice the length of the member thickness.

The simulation results show that the relationship between the angle increase and the CTE increase produces and more stable rate of change between each angle after 60°. This is because as we reduce the angle below 60° the movement moves away from being stretch dominated to bend dominated, and the displacements that would otherwise be created and translated into stresses inside the members. Therefore a design engineer should look to choose a member thickness that places the desired CTE plotted within 60° to 75°.

Primary Material	Secondary Material	CTE Ratio	Member Thickness (L)	Lattice Angle (θ)	Probe 1 CTE (E-06)	Probe 2 CTE(E-06)	Stiffness (MPa)	Specific Stiffness ($E^{4}m^{2}s^{-2}$)	Weight (g)
Titanium	INVAR	1:6.6	3mm	60°	-5.8	2.9	94	2.0	92.9
				75°	-4.4	2.9	145	3.1	
			1mm	60°	-7.5	2.3	30	0.6	63.75
				75°	-5.2	2.3	49	1.1	
Stainless Steel	Titanium	1:1.6	3mm	60°	10.5	11.3	129	1.6	127.52
				75°	10.6	11.3	199	2.5	
			1mm	60°	10	11.2	40	0.5	73.4
				75°	10.3	11.2	66	0.8	
Aluminium	Titanium	1:2.5	3mm	60°	1.5	13.8	92	3.4	54.24
				75°	3.4	13.8	140	5.2	
			1mm	60°	-1.5	12.7	28	1.1	36.75
				75°	1.8	12.7	47	1.8	
Aluminium	Stainless Steel	1:1.9	3mm	60°	1.6	13.9	95	3.4	67.8
				75°	3.7	13.9	147	5.3	
			1mm	60°	-0.37	13.2	30	1.1	50.32
				75°	2.8	13.2	49	2.0	

Table 1) Show simulation CTE results for Design 1 from a range of material combinations.

The table above shows the different CTE values obtained through simulation, for the corresponding materials and lattice angle. The CTE for the simulation has been taken from our testing shown in table 2. The specific stiffness is also called the stiffness to weight ratio, where weight is divided by its corresponding stiffness. This provides us with an idea of the effectiveness of the solution at keeping a lightweight design whilst remaining stiffness. The difference CTE between values at probe 1 and probe 2 provide a measure of effectiveness for the lattice structure. A higher difference implies more work done by the structure to reduce the CTE. Typically, this will be most effective where a high CTE material is present as the primary material. Aluminium coupled with Titanium or Steel as a secondary material is a good example, reducing the CTE of a conventional solid ring from $24x10^{-6}$(1/K) to $-1.5x10^{-6}$(1/K) when L=1mm and θ=60°. A good choice of material is one where the combination provides the required CTE in between the range of angle, or range of thickness depending on stiffness required.

Materials and Experiment

To verify designs created through simulation data, the structures need to be manufactured and tested for performance. To ensure the most accurate simulations, the CTE of LPBF parts have been measured. This data has been fed back into the simulation as material data. It is important to measure the CTE of parts manufactured using LPBF because the CTE will differ from that of the corresponding material manufactured through traditional means. Certain parameters such as build direction and porosity have all been shown to affect the thermal expansion of a component [13][14][7]. The CTE of the entire lattice structure also needs to be considered.

Dilatometer Measurements

To successfully simulate and manufacture a structure capable of changing the CTE, first an understanding of the CTE of printed parts on a LPBF machines is required. Two LBPF machines are available at Swansea University, a Renishaw AM250 which utilises a 200W 1070nm Yb fibre optic laser with a laser scanning speed of up to 2m/s, and a RenAM500 which utilises a 500W laser with a similar bed size and scanning characteristics. Using the AM250 several dilatometer roads (6mm diameter x 25mm length) were built in vertical and horizontal orientations. The rods were tested using a NETZSCH 402 dilatometer featuring a

cryogenic furnace capable a temperature range of -200°C and +1000°C. These results are given in table 2 for a temperature range of -70°C and +100°C from a sample size of -100°C to +130°C. Trimming 30°C off both extremities removes noise from the data set.

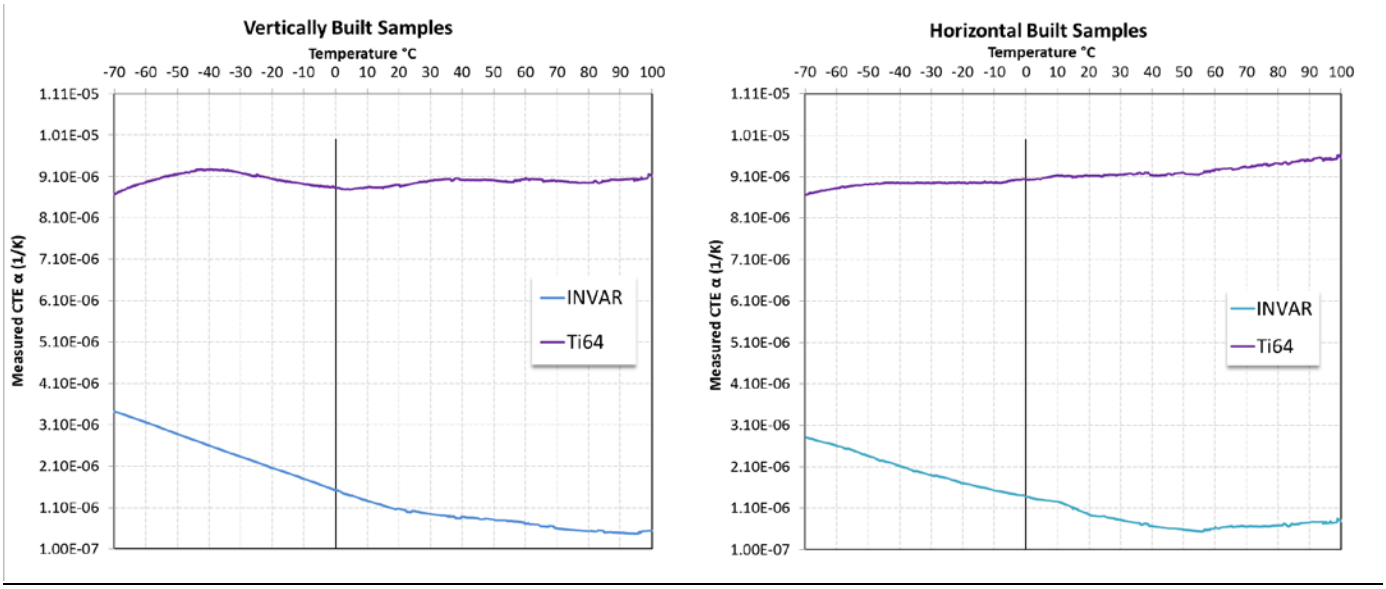

Figure 8) Graphs showing the CTE against temperature built vertically and horizontally. Measured using the NETZSCH 402 Dilatometer.

Material	Temperature Range	H CTE	V CTE	Averaged CTE
Titanium Ti64Al	-70°C to +100°C	$9.12x10^{-6}$(1/K)	$9.00x10^{-6}$(1/K)	$9.06x10^{-6}$(1/K)
INVAR	-70°C to +100°C	$1.31x10^{-6}$(1/K)	$1.50x10^{-6}$(1/K)	$1.41x10^{-6}$(1/K)
Aluminium [15]	25°C to 200°C	N/A	N/A	$24x10^{-6}$(1/K)

Table 2) Shows dilatometer results for INVAR and Ti64Al using the Renishaw AM250, and Renishaw RenAM500 LPBF Machine respectively. Aluminium is referenced from another source.

This data is very important to determining the most effective method of controlling CTE. It can be seen that the CTE for INVAR increases as the temperature decreases. This is different to the CTE for Ti64Al which decreases as the temperature decreases. This will need to be taken into account with any CTE offsetting design. Heat treatment of the part can change the thermal expansion values, but for this experiment we are looking at as built.

Results and Discussion

It is observed that an optimum lattice angle for the proposed design is between 60-75degrees. It is observed that the stiffness is increased greatly as the member thickness (L) is increased, but the CTE only decreases marginally. This is due to the cross-member lengths La being twice that of L. The force created from the expansion of adjoining members (La) must overcome equally the additional thickness of members (L). Optical engineers will be able to choose an angle, thickness (L), and material combination from experimentation following the design rules proposed. It can be seen that the high specific stiffness of $5.2.E^{4}.m^{2}\ s^{-2}$ for aluminium made it a great choice for lightweight applications. The combination of aluminium and titanium in the proposed lattice structure features one of the highest reductions in CTE from 24×10^{-6}(1/K) to -1.5×10^{-6}(1/K).

Conclusion

Modelling shows that an auxetic lattice of a single material coupled with an external containing ring can be used to create customized coefficients of thermal expansion around a 2D annulus. This opens the possibility of matching CTE's within an optical system to the lens material. It has shown that a design engineer can follow a set of design rules regarding member thickness and lattice angle to achieve the desired co-efficient of thermal expansion. Negative CTE's have been achieved when using a high CTE ratio such as INVAR and titanium. Further work is required to test the designs and ensure they match the simulation data. The future multi-material print requires further work in manufacturing with Fused Deposition Modelling (FDM) polymer machines featuring different amounts of carbon and glass fibres. A DED LENS system will also be explored for making a multi-metallic print.

Acknowledgements

This research was supported by Sêr Cymru funding through the National Research Network in Advanced Engineering and Materials in Wales (grant NRN145) and by Qioptiq. The authors would like to thank the Welsh European Funding Office and the Welsh Government for the funding which enabled the Materials Advanced Characterisation Centre (MACH1) and the Advanced Sustainable Manufacturing Technologies (ASTUTE 2020).

References

[1] "Thales Alenia Space, the world champion in 3D-printed parts in orbit! | Thales Group." [Online]. Available: https://www.thalesgroup.com/en/worldwide/space/press-release/thales-alenia-space-world-champion-3d-printed-parts-orbit. [Accessed: 13-Jun-2017].

[2] M. Seabra *et al.*, "Selective laser melting (SLM) and topology optimization for lighter aerospace componentes," *Procedia Struct. Integr.*, vol. 1, pp. 289–296, 2016.

[3] G. Imbalzano, P. Tran, T. D. Ngo, and P. V. S. Lee, "A numerical study of auxetic composite panels under blast loadings," *Compos. Struct.*, vol. 135, pp. 339–352, 2016.

[4] Q. Yang, S. Meng, W. Xie, H. Jin, C. Xu, and S. Du, "Effective mitigation of the thermal short and expansion mismatch effects of an integrated thermal protection system through topology optimization," *Compos. Part B Eng.*, vol. 118, pp. 149–157, 2017.

[5] J. Mazumder, *1 - Laser-aided direct metal deposition of metals and alloys*. 2017.

[6] "Properties of KOVAR."

[7] C. Qiu, N. J. E. Adkins, and M. M. Attallah, "Selective laser melting of Invar 36: Microstructure and properties," *Acta Mater.*, vol. 103, pp. 382–395, 2016.

[8] X. C. Li, J. Stampfl, and F. B. Prinz, "Mechanical and thermal expansion behavior of laser deposited metal matrix composites of Invar and TiC," *Mater. Sci. Eng. A*, vol. 282, no. 1–2, pp. 86–90, Apr. 2000.

[9] R. LAKES, "Foam Structures with a Negative Poisson's Ratio," *Science (80-.).*, vol. 235, no. 4792, pp. 1038–1040, Feb. 1987.

[10] C. A. Steeves, S. L. dos Santos e Lucato, M. He, E. Antinucci, J. W. Hutchinson, and A. G. Evans, "Concepts for structurally robust materials that combine low thermal expansion with high stiffness," *J. Mech. Phys. Solids*, vol. 55, no. 9, pp. 1803–1822, 2007.

[11] O. Sigmund and S. Torquato, "Design of Materials With Extreme Thermal Expansion Using a Three-Phase Topology," *J. Mech. Phys. Solids*, vol. 45, no. 6, pp. 1037–1067, 1997.

[12] Q. Yang, S. Meng, W. Xie, H. Jin, C. Xu, and S. Du, "Effective mitigation of the thermal

short and expansion mismatch effects of an integrated thermal protection system through topology optimization," *Compos. Part B Eng.*, vol. 118, pp. 149–157, 2017.
[13] C. A. Steeves, C. Mercer, E. Antinucci, M. Y. He, and A. G. Evans, "Experimental investigation of the thermal properties of tailored expansion lattices," *Int. J. Mech. Mater. Des.*, vol. 5, no. 2, pp. 195–202, 2009.
[14] A. V. Pozdniakov *et al.*, "Development of Al-5Cu/B4C composites with low coefficient of thermal expansion for automotive application," *Mater. Sci. Eng. A*, vol. 688, pp. 1–8, 2017.
[15] K. Olakanmi, EO, Cochrane, RF and Dalgarno, "A review on selective laser sintering/melting (SLS/SLM) of aluminium alloy powder: Processing, microstructure, and properties.," 2015.